Significant Low-Order Effects in the Onset of Protonation and Related Interactions

Clifford E. Dykstra*

Department of Chemistry, Indiana University−Purdue University Indianapolis, 402 North Blackford Street, Indianapolis, Indiana 46202

Received: December 21, 2002; In Final Form: March 17, 2003

Ab initio calculations have been performed for hydrogen fluoride, water, and formaldehyde to understand the influence of an approaching point charge or a point dipole. As a function of the separation distance between the molecule and the point charge multipole, response properties through as high as the seventh order were calculated. The response properties were used to evaluate the interaction energy order by order for charges and dipoles of specific sizes, and these energies were compared with the fully evaluated interaction energy. Through a considerable range of approach distance, low-order reponse properties were sufficient to yield an accurate interaction energy. Even the second-order treatment was suitable over a sizable range. This result is useful for interpreting interaction effects for charged species. It is also useful for constructing model potentials for ion approach to neutral molecules and for respresenting the long-range parts of proton exchange potentials.

Introduction

There is considerable theoretical insight and calculational information about protonation of small organic molecules and about the strong type of hydrogen bonding wherein a proton takes on the role of a bridging atom,[1] as in $H_5O_2^+$, for instance.[2−4] Generally, the presence of a species with a net charge, either positive or negative, leads to a more sizable long-range interaction with any approaching molecule than would an uncharged species. Hence, for a protonated species, a cation, the type of hydrogen bonding in which it can participate seems quite different from the weak hydrogen bonding that may take place among neutral species, such as that in $(H_2O)_2$. A proton bridge between molecules can have the strength usually associated with chemical bonds, whereas that is not likely for hydrogen bonds among a pair of neutral molecules. The presence of a net charge, then, is significant. Given that, it is interesting to analyze the extent to which features of weak hydrogen bonding among neutrals carry over to protonated systems. This study addresses part of that issue by examining, via perturbation theory, the effects of a point charge on three small molecules, contrasting and comparing that in one case with the effects of a point dipole which can be an influence in the absence of a net charge (i.e., the influence of a neutral). Throughout, low-order perturbation theory analysis provides a remarkably good accounting of the interaction energetics.

Perturbation theory energies for the influence of a fixed point charge or other point multipole have an order-by-order association with properties. The first-order energy is the interaction of the molecule's entire set of permanent moments with the point multipole. The second-order energy is the polarization energy, while the third-order contribution is due to hyperpolarization. Normally, molecular (hyper)polarizabilities are formed as responses to fields, field gradients, and so on. The dipole polarizability tensor α yields the dipole induced by a uniform field, the quadrupole polarizability C yields the quadrupole induced by a field gradient, and so on.[5] The electrostatic potential of a point multipole can be expressed as a power series expansion in spatial coordinates with the factors in the series being uniform field components, field gradient components, and so on, used in forming the conventional response properties. In this way, the (hyper)polarization response to a point multipole is implicitly an infinite sum involving these conventional response properties. In particular, for a point charge (or zeroth-order multipole) q located in space at (x,y,z) acting on a molecule at (0,0,0), the polarization energy is

$$E_{\text{polariz}} = -\frac{1}{2}q^2\left(\alpha_{xx}\frac{x^2}{r^6} + \alpha_{yy}\frac{y^2}{r^6} + \alpha_{zz}\frac{z^2}{r^6} + \alpha_{xy}\frac{xy^2}{r^6} + \ldots \right.$$
$$\left. 2A_{x,xx}\frac{x(2x^2 - y^2 - z^2)}{r^8} + \ldots\right) \quad (1)$$

where α is the dipole polarizability, A is the dipole−quadrupole polarizability, r is $(x^2 + y^2 + z^2)^{1/2}$, and the sum continues through all multipole polarizabilities conventionally defined. In practice, this expansion is truncated, sometimes with only α-terms. However, for the strong effects of a point charge, the adequacy of a chosen level of truncation is a concern. This can be circumvented formally by simply recasting the response properties via a straightforward, textbook-level step. Instead of defining them as responses to the pieces in a spatial power series expansion of an arbitary external potential (i.e., as responses to a field, field gradient, etc.), the response can be defined in terms of external multipoles. The polarization energy of a point charge q is then

$$E_{\text{polariz}} = -\frac{1}{2}q^2P_{00} \quad (2)$$

with P_{00} being the polarizability value associated with the external influence of a zeroth-order multipole (point charge). Because P_{00} is equal to what is inside the outermost parentheses in eq 1, it is clear that P_{00} has a geometrical connection to the external perturbation that α, A, C, and the other conventional polarizabilities do not; i.e., $P_{00} = P_{00}(x,y,z)$. At any given spatial position (x,y,z) of the perturbing charge, P_{00} can be evaluated by ab initio methods, and in so doing, no truncation over conventional multipole polarizabilities is required. The informa-

10.1021/jp022651i CCC: $25.00 © 2003 American Chemical Society
Published on Web 04/29/2003

TABLE 1: One-Electron Operators[a] and Peturbative Parameters for Response Properties

	conventional form		point multipole form	
multipole order	operator (potential, field, gradient)	parameter	operator (charge, dipole, quadrupole)	parameter
0	$\sum_i q_i$	V_0	$\sum_i (q_i/r_{pt-i})$	q_{pt}
1	$\sum_i q_i x_i$	V_x	$\sum_i (q_i x_i/r^3_{pt-i})$	μ_{pt-x}
	$\sum_i q_i y_i$	V_y	$\sum_i (q_i y_i/r^3_{pt-i})$	μ_{pt-x}
	$\sum_i q_i z_i$	V_z	$\sum_i (q_i z_i/r^3_{pt-i})$	μ_{pt-x}
$2(xx)^b$	$^1/_2\sum_i q_i x_i^2$	V_{xx}	$\sum_i q_i[(-1/r^3_{pt-i}) + (3x^2/r^5_{pt-i})]$	Q_{xx}
$N(x^N)^b$	$^1/_2\sum_i q_i x_i^N$	V_{xN}	$\sum_i q_i(\partial^N/\partial x^N_{pt-i})(1/r_{pt-i})$	M_{xN}

[a] The sums over the index i are over the electrons and the nuclei in the molecule. [b] Conventional mutipole operators are given in Cartesian form and can be transformed to spherical form.

tion contained in the infinite set of conventional multipole polarizabilities is thereby mapped into a representation, one with an infinite number of values due to the geometry dependence. The first task of this report is to show, in part, the nature of that geometry dependence for a few small molecules.

In addition to P_{00}, there must exist polarizabilities associated with point multipoles of order greater than zero and, with that, come mixed multipole polarizabilities analogous to a dipole−quadrupole polarizability, for instance, in the conventional set of response properties. For convenience, we shall adopt/extend Applequist's polytensor organization[6] in distinguishing these properties. That is, an index value of 0 means a point charge, 1 means the *x*-component of a point dipole, 2 means the *y*-component, and 3 means the *z*-component. The index 4 means the *xx*-component of a perturbing point quadrupole, 13 means the *xxx*-component of a point octupole, and so on. Hence, the recast set of polarizabilities will include P_{01}, P_{11}, P_{02}, P_{12}, P_{22}, and so forth, with the two indices corresponding to two index values from the multipole list. The first hyperpolarizabilities will have three indices.

To find the P_{nm} properties by ab initio calculations, one-electron operators that correspond to the perturbations are needed. For conventional properties, we might start with a uniform field in the *x*-direction V_x, which gives a perturbing Hamiltonian,

$$H^{(1)} = -V_x \mu_x \tag{3}$$

where μ_x is the usual dipole moment operator, a one-electron operator whose matrix representation can be readily evaluated in a basis set of Gaussian atom-centered functions in typical ab initio calculations. For an external point charge q_{pt}, the perturbing Hamiltonian is

$$H^{(1)} = -q_{pt} \sum_i \frac{q_i}{r_{pt-i}} \tag{4}$$

The sum is over the charges q_i in the molecule, the electrons, and nuclei, and r_{pt-i} is the distance from q_{pt} to the ith charge in the molecule. A matrix representation of this operator in a basis of Gaussian functions is a standard evaluation, one normally done to give the electrostatic potential at the (x,y,z) location of q_{pt}. For both types of response properties, the necessary one-electron operators can be generated to any order.[7] Table 1 lists the form for several of lowest order.

For any $H^{(1)}$ associated with an external electrical influence, there is a parameter that multiplies a given one-electron operator, such as those operators in Table 1. The derivatives of the molecular eigenenergy with respect to these parameters are the response properties. Second derivatives are polarizabilities. Third derivatives are the first hyperpolarizabilities. Table 1 shows the parameters that are associated with each operator.

For some parameter ρ, a series expansion of the molecular eigenenergy is

$$E = E(\rho{=}0) + \rho \left.\frac{\partial E}{\partial \rho}\right|_{\rho=0} + \frac{1}{2}\rho^2 \left.\frac{\partial^2 E}{\partial \rho^2}\right|_{\rho=0} + \frac{1}{6}\rho^3 \left.\frac{\partial^3 E}{\partial \rho^3}\right|_{\rho=0} + \ldots \tag{5}$$

The energy derivatives are the response properties, e.g., $(\partial^3 E/\partial \rho^3)|_{\rho=0}$. The perturbation theory equivalent of eq 5 is

$$E = E^{(0)} + \rho E^{(1)} + \rho^2 E^{(2)} + \rho^3 E^{(3)} + \ldots \tag{6}$$

The perturbation corrections to the energy are directly obtained via the response properties. While the details of the special response properties being used here need to be clearly identified, there is nothing novel or even complicated in working with this form. Of importance is that using the point multipole response properties instead of a truncated set of conventional properties removes their truncation error. That in turn is essential to assess perturbation theory treatment order by order. What develops is a useful perspective on interactions where there is a charged species. The results from the calculations show that, with no more than the ρ^2 term in eq 6, long-range interaction energies as strong as around 30 kcal/mol are well reproduced. Going to truncation at third order extends the range over which the energies are well reproduced much more. Such simplicity implies the means for constructing potentials and for representing parts of interaction surfaces concisely.

Calculational Approach. All calculations employed the doubly augmented correlation consistent bases, aug-2-ccpVTZ.[8] An initial set of calculations was done for a proton approaching hydrogen fluoride along the H−F axis from one side and then from the other. Hydrogen basis functions were used at the approaching proton center. The bond length of HF was fixed at 0.92 Å. The correlation effect was evaluated at the MP2[9,10] and at the coupled cluster[11−15] level of single and double substitutions (CCSD) using a minor approximation[16,17] that has been shown to be very faithful to the nonapproximate form.[18] Figure 1 compares the relative or interaction correlation energies from MP2 and the coupled cluster treament for both approaches. Differences at long range are very small, and even in the very close-in region where there is the worst deviation in the curves, the higher level treatment changes the total interaction energy by less than 2%. Furthermore, as the selected values in Table 2 show, the correlation contribution from MP2 evaluation remains quite small until the total interaction energies become greater in size than roughly 100 kJ mol^{-1}.

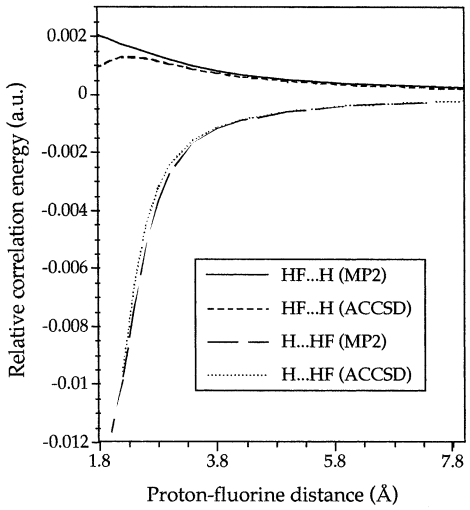

Figure 1. For the collinear approach of a proton to hydrogen fluoride, the correlation energy is shown relative to that at infinite separation (i.e., the intereaction correlation energy). Curves are given for correlation energy obtained at the MP2 level and at a more extensive level of coupled cluster theory (CC). The correlation effect is more sizable for approach of the proton to the proton end of HF, but it is smaller throughout than the SCF energy changes.

TABLE 2: Examples of the Sizes of the Counterpoise Corrections and Relative Interaction Energies for Collinear Approach of a Proton to Hydrogen Fluoride, HF···H$^+$

	counterpoise correction (au)		interaction energy	
F−H$^+$ separation[a] (Å)	SCF energy	MP2 correlation energy	total (kJ mol^{-1})	% from correlation (MP2)
−3.4	0.000017	0.000002	61.3	7.2%
−2.8	0.000025	0.000023	85.2	12.3%
−2.2	0.000053	0.000048	103.4	25.0%
2.0	0.000070	0.000220	−116.1	−1.8%
3.0	0.000014	0.000037	−44.6	−6.7%

[a] Negative separation distances correspond to H$^+$−HF structures, whereas positive values correspond to HF−H$^+$.

The primary effect of a proton approaching HF develops at the SCF level. For both axial approach directions, the correlation effects on the interaction energy are in the direction of offsetting part of the SCF interaction energy. We also note from the values in Table 2 that the lingering basis set superposition error is small. Counterpoise correction was performed in every calculation, but with the basis used, the corrections are tiny.

Following the calulcations on HF, like calculations (SCF and MP2 with the aug-2-ccpVTZ basis) were performed for a point charge approaching formaldehyde and approaching water. The fixed geometry of formaldehyde from an ab initio calculation[19] was 1.111 Å for the CH bond length, 1.205 Å for the CO bond length and 116.1° for the HCH angle. The approach direction for the proton was toward the oxygen, collinear with the C−O bond. The geometry for water was 0.957 Å for the bond length and 105.2° for the angle, and the proton approach was along the C_2 symmetry axis toward the oxygen.

Derivative Hartree−Fock (DHF) calculations[20] were performed for hydrogen fluoride, for formaldehyde, and for water to find response properties at the SCF level for a point charge at a given position in space relative to the molecule. This is readily done by finding the one-electron operator for a point charge while taking the size of the charge to be the variable of response (parameter). That is, the DHF scheme was used in this type of a calculation to analytically evaluate the first derivative, second derivative, third derivative, and so on, with respect to the amount of charge at the point.

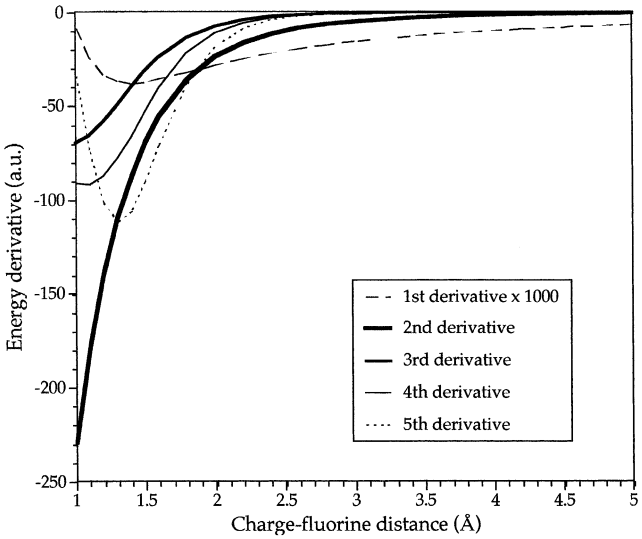

Figure 2. Dependence of low-order derivatives (au) of the SCF energy of HF with respect to the amount of charge q placed along the HF axis. The point charge approach corresponds to (a) HF-q and (b) q-HF.

A further set of calculations was performed for hydrogen fluoride experiencing a point dipole instead of a point charge. A generalized operator program[7] was used to obtain the one-electron operator matrix for a point dipole in the Gaussian basis, and DHF calculations were performed to yield the associated response properties. Then, SCF and MP2 calculations were carried out with that one-electron operator multiplied by a value of 1 au (2.5418 D) and added to the one-electron part of the Hamiltonian. This procedure yields an evaluation of the full interaction energy for an approaching dipole of 1 au.

Results and Discussion

The calculated response properties of hydrogen fluoride to an approaching point charge collinear with the H−F axis are shown in Figure 2. The first derivative curve corresponds to interaction of a point charge with the permanent charge field of the molecule. At long range, this is attractive from one end and repulsive from the other. The curves for the higher order derivatives show mostly an increase in their size as the separation distance from the molecule is diminished. To show how these properties contribute to the interaction energy via eq 5, we select +1 as a representative size of an approaching charge, i.e., a proton, and apply eq 5 order by order. Figure 3 shows a comparison of the results of SCF evaluation of the energy of a proton interacting with HF and the results of an evaluation based on the DHF response properties displayed in Figure 2. The energy through second order, which is with the inclusion of P_{00}, nicely follows the complete interaction curve at the SCF level through interaction strengths of 130 kJ mol^{-1}. Over this range, the expansion is essentially converged by fifth order. (Treatments through third and fourth orders are not shown because of congestion in the plot, but both curves lie between the second- and fifth-order curves.)

Qualitatively similar to the results for a point charge approaching HF are the results for a point charge approaching the oxygen end of formaldehyde. While the fifth derivative response property of H_2CO has minimum at a close-in distance of about 1.3 Å in the charge−oxygen separation, the response properties otherwise increase in size with decreasing distance at least down to a separation of 1 Å. They are not unlike the

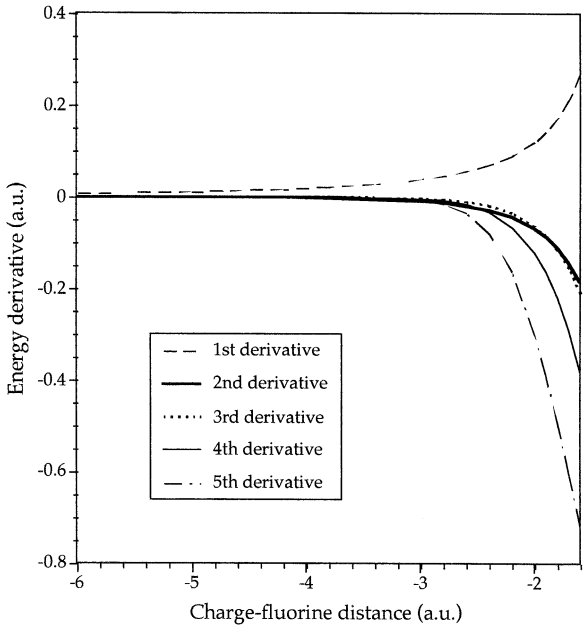

Figure 3. SCF interaction energy (au) for a proton collinear with HF is shown along with an evaluation of the energy based on point-charge response properties. These evaluations are through the second, fifth, and seventh orders and are shown for the region in which the size of the interaction energy is up to about 150 kJ mol^{-1}. The proton position relative to the fluorine corresponds to (a) $HF-H^+$ and (b) H^+-HF.

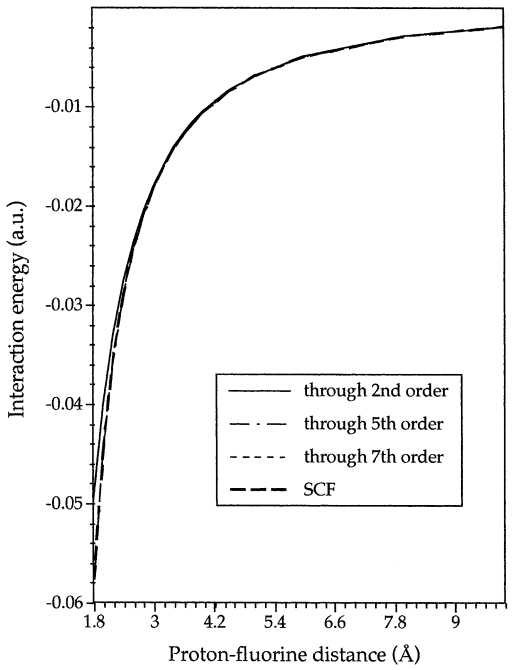

Figure 4. SCF interaction energy (au) for a proton approaching formaldehyde along the C−O axis is shown along with an evaluation of the energy based on the point-charge response properties. These evaluations are through the second, third, and fourth orders.

properties shown in Figure 2 for the approach of the point charge to the fluorine end of HF. Interaction energies for H_2CO shown in Figure 4 compare the eq 5 expansion with the full interaction at the SCF level. The adequacy of a second-order treatment is similar to that for HF, with higher orders rapidly converging to the SCF interaction.

The comparisons of the perturbative expansions have been with SCF energies because the derivatives are readily evaluated at the SCF level and because the correlation effect has a small

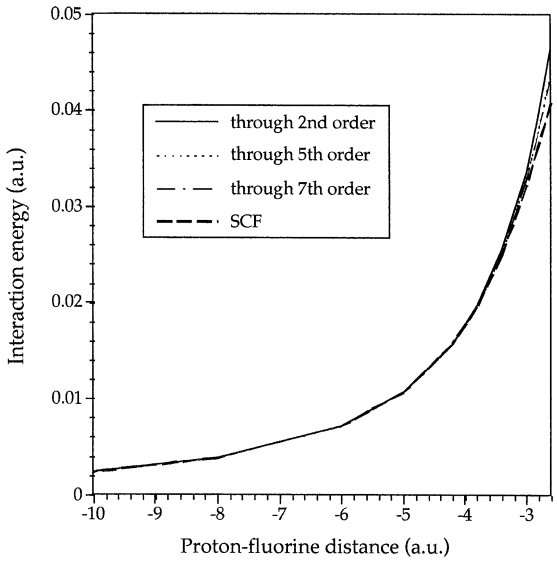

Figure 5. Energy of interaction for the approach of a proton to formaldehyde along the CO axis and from the oxygen side is shown at the SCF level and with correlation energy from MP2 included. The correlation energy provides only a small refinement of the interaction from far out to as close as 1 Å.

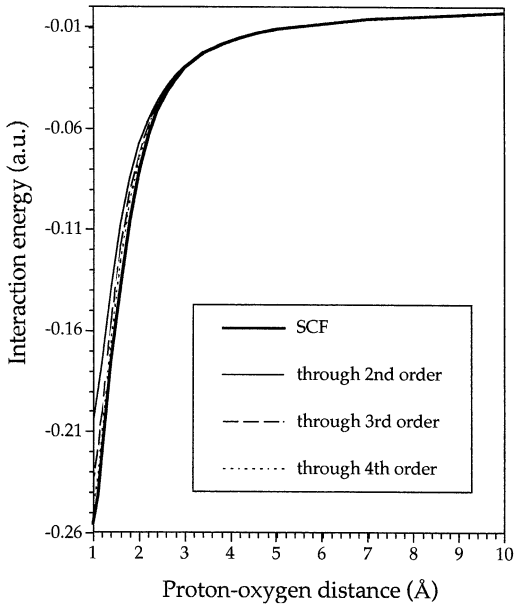

Figure 6. Energy of interaction of HF for the approach of a point dipole that is 1 au in size and aligned with the molecular axis is shown at the SCF level and with correlation energy from MP2 included.

role. This is apparent by comparing the correlation contributions to the interaction energy for HF in Figure 1 with the SCF interaction energies in Figure 3 and again for H_2CO by the comparison in Figure 5. Though the focus here is on the SCF interaction, nothing precludes working with correlated response properties as a way of recovering the small correlation part of the interaction.

The next step is comparison with a point dipole. This is a perturbation which can be associated with approach of a neutral molecule since there is no net charge. Of course, it is not a complete representation of a real molecule nor is it meant to be. The idea is to compare influences that are alike in the sense of being point multipoles. Figure 6 shows SCF and correlated interaction curves for a dipole of 1 au size aligned with the molecular axis and approaching HF from the fluorine end. There

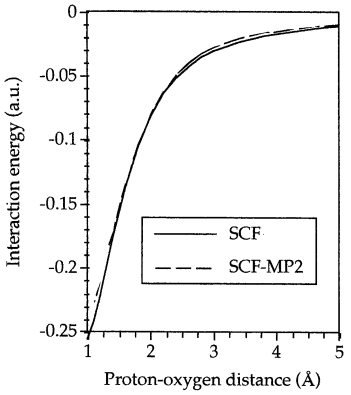

Figure 7. Dependence of low-order derivatives (au) of the SCF energy of hydrogen fluoride with respect to the size of a point dipole μ_x placed along and aligned with the HF axis and on the fluorine end of the molecule.

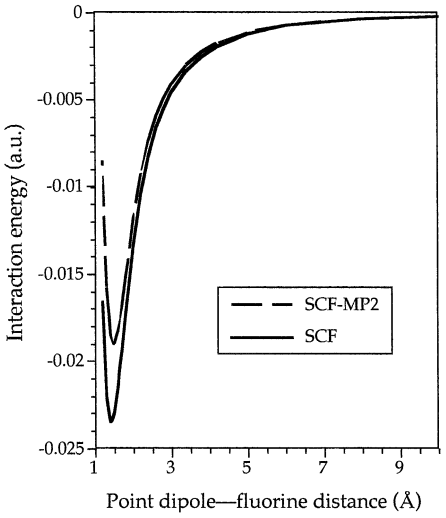

Figure 8. SCF energy of interaction of HF for the approach of a point dipole 1 au in size aligned with the molecular axis and on the fluorine end is shown along with an evaluation based on point-dipole response properties.

is a minimum in the interaction curve, and correlation effects, though small, are most noticeable in the region around this minimum. The DHF response properties for a point dipole are shown in Figure 7 and the results of applying an order-by-order perturbative treatment are in Figure 8. The first-order curve has the qualitative behavior of the full interaction, but the quantitative reliability stands out at second order with essentially a converged result at third order.

With the result that the role of the low-order response is similar for a molecular-sized point dipole as for the relatively drastic influence of a point charge, it is useful to examine in greater detail certain of the differences. Figure 9 gives a closer view of that displayed in Figure 3a but with the interaction of the approaching point charge and the permanent charge field of the molecule removed (i.e., without the first-order energies). This isolates the polarization and hyperpolarization contribution to the interaction. The error of the second-order treatment is clearly seen to develop close-in. Inclusion of the third-order response (first hyperpolarizability P_{000}) brings the curve a step closer to the full interaction curve based on the SCF energies. Another curve in Figure 9 is that obtained by evaluating the

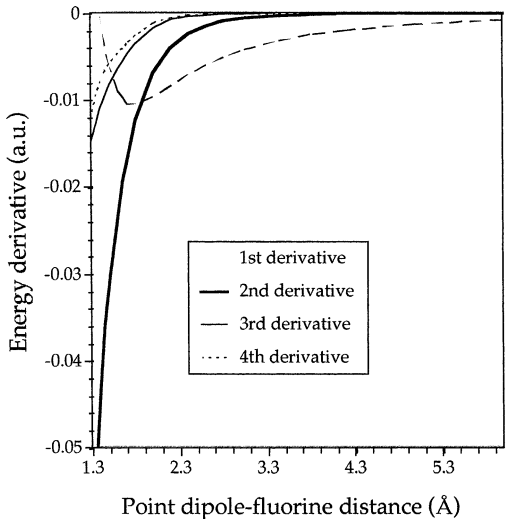

Figure 9. Part of the interaction energy (au) not associated with the permanent charge field of HF is shown for a proton collinear with the molecule and on the fluorine end. This part of the interaction energy has been evaluated completely at the SCF level (heavy solid curve) by subtracting the permanent charge field interaction, which is the first-order perturbation theory energy, from the SCF energy. The second-order energy is shown with a light, solid curve. (This energy combined with the first-order energy is in Figure 3a.) The sum of the second- and third-order energies is shown by a broken line. The second-order energy based on using the conventional dipole polarizability only, not on the point charge response property, is shown by the dashed line.

polarization energy that arises from an approaching point charge via the conventional dipole polarizability α. This curve is not seriously in error, and the use of α alone in interaction models even involving charged species has some attributes. However, the shape of the curve differs from the other three. This is because it descends too quickly as the approach distance decreases. At the same time, for part of the evolution of the protonation process, this overvaluing of the polarization energy makes up for the neglect of the energy associated with hyperpolarization. In developing potential models, there is always some tradeoff between complexity of the potential and accuracy,[21] and hence, there are certainly applications where models incorporating no more than the response associated with α are reasonable and appropriate.

The fact that the energetics of charge and dipole approach to a neutral closed shell molecule are well reproduced via low-order response properties suggests a model for interaction potentials on the basis of simply selecting a truncation point in the order of response included. One possible application of such modeling is in the potential surfaces for proton exchange between two neutral molecules, e.g., A···H^+···B. If response properties for A and B are in hand, then using them for the A···H^+···B system in the simplest modeling effort (second order) amounts to treating the A···H^+ and H^+···B interactions as additive. Test calculations using A = B = water show how well this additivity approximation holds, and the results are given in Figures 10 and 11. In these calculations, two water molecules were arranged in a plane so as to have C_{2v} or D_{2h} symmetry with the oxygen ends toward each other, i.e., H_2O-OH_2. There are a number of high-level ab initio calculations,[2−4,22−26] and out of these, the equilibrium structure of $H_2O_5^+$ is known to be of lower symmetry (nonplanar); however, the planar constraint used here includes a representative surface region with substantial interaction, and this higher symmetry has a computational advantage. Results shown in Figure 10 are the interaction

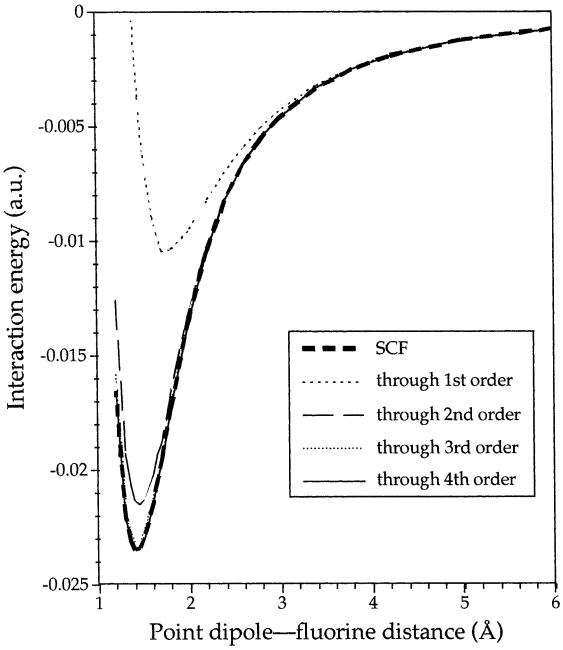

Figure 10. The interaction energy (au) for a proton placed between two water molecules with an overall D_{2h} symmetry structure. The horizontal axis is the distance of the proton from either oxygen atom. The energy designated "full" is the ab initio energy of the $H_5O_2^+$ cluster less the energy of the cluster without the central proton, i.e., a water dimer structure. The other energy is twice the ab initio interaction energy corresponding to the arrangement of a proton and a water molecule as in the $H_5O_2^+$ cluster. This is the energy of a proton interacting with two waters independently.

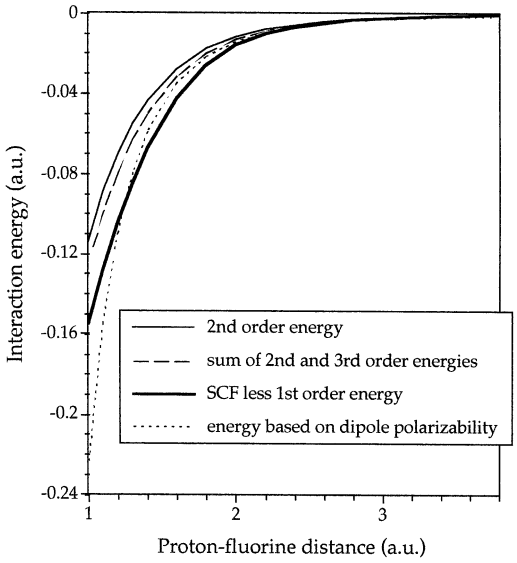

Figure 11. The interaction energy (au) for a proton placed between two water molecules with an overall C_{2v} symmetry structure. The oxygen−oxygen separation distance is 6 Å in the upper two curves and 5 Å in the lower two curves. The horizontal axis is the distance of the proton from the midpoint of the line between the two oxygen atoms. The energy designations are the same as in those in Figure 10.

energy curves for a proton placed symmetrically between the two waters with D_{2h} symmetry maintained. Results shown in Figure 11 are for fixed oxygen−oxygen separations of either 5 or 6 Å with the proton's position varying from one side to the other. In both figures, there is a curve showing the SCF interaction energy ("full") and a curve based on independent (SCF) evaluations of the proton interacting with each water ("indep. int."). The latter curve is the sum of the interaction energies calculated for a proton with the left-side water and a proton with the right-side water, these energies being the ones that can be very well reproduced via low-order response properties. The extent of additivity, or independence, of the interactions is shown by the curve in Figure 10 labeled "difference" and by the closeness of the pairs of curves in Figure 11. The nonadditive parts remain as a small share over a considerable range of interaction with the significant growth of nonadditive pieces occurring as the waters become close. Notice from Figure 11 that, with proton interaction energies of as much as 700 kJ mol^{-1}, nonadditivity happens to remain small. On the other hand, the information in Figure 10 shows that this is so only for relatively long water−water separations. When the oxygens of the waters are 3 Å apart in a D_{2h} structure, the nonadditivity is approaching a fourth of the interaction strength.

We cannot argue that the nonadditive parts of the proton bridging interaction in the water−water cluster are ignorable, because they eventually do become sizable with closer separations. However, for the purpose of developing potential surfaces to describe proton transfer, it seems clear that there are extensive regions, both in terms of interaction energy and spatial dimensions, where the proton's interaction with monomer subunits is so nearly additive that very simple modeling is likely to be effective. Furthermore, part of the source of nonadditivity, the mutual electrical interaction of the monomers on being polarized by the bridging proton can be included easily in a model. Most important at this stage is that the results point to a compact representation for a protonation potential at long range. In practice, a second- or third-order potential could be spliced to a fully evaluated, close-in ab initio potential at some appropriate distance. This would ensure an accurate form for the potential without explicit ab initio calculations for the long-range parts.

The calculations reported here show that rather low order of response provides good potentials. All that is necessary are response properties, and low-order ones at that, for isolated molecules. There is, therefore, usefulness in collecting these properties for small molecules where there are interesting proton-bridging systems, such as certain amino acids.

Conclusions

Correlation effects on the protonation potential of $HF-H^+$ and H_2CO-H^+ are small. Especially at long range, the dominant part of the interaction, is via the SCF energy. SCF response properties through only the second order (i.e., polarization) were found to describe the interaction in the test molecules HF, H_2O, and H_2CO for an approaching point charge at long range. The onset of protonation clearly starts as a simple electrostatic response, and this means that it can be modeled in rather simple form. In that, the approach of a point dipole instead of a proton develops similarly. Casting the response properties in terms of point multipole responses rather than the more conventional field/field gradient responses strictly isolates the order-by-order effects and shows the effectiveness of low-order analysis. Significant in this work is a good amount of additivity of the proton interaction in the $A\cdots H^+\cdots B$ system of A = B = water. That helps in using low-order response properties intrinsic to the molecules to model the $A\cdots H^+\cdots B$ proton-transfer potential. Combined with models for long-range, weak interaction among neutral species, e.g., A···B potentials, complete model schemes for proton bridging in large aggregations may result.

Acknowledgment. This work was supported, in part, by a grant from the Physical Chemistry Program of the National Science Foundation (CHE-0131932).

References and Notes

(1) Scheiner, S. *Hydrogen Bonding−A Theoretical Perspective*; Oxford University Press: Oxford, 1997.
(2) Xie, Y.; Remington, R. B.; Schaefer, H. F. *J. Chem. Phys.* **1994**, *101*, 4878.
(3) Ojamae, L.; Shavitt, I.; Singer, S. J. *Int. J. Quantum Chem.* **1995**, *S29*, 657.
(4) Edison, A. E.; Markley, J. L.; Weinhold, F. *J. Phys. Chem.* **1995**, *99*, 8013.
(5) Buckingham, A. D. *Adv. Chem. Phys.* **1967**, *12*, 107.
(6) Applequist, J. *J. Math Phys.* **1983**, *24*, 736; *Chem. Phys.* **1984**, *85*, 279.
(7) Augspurger, J. D.; Dykstra, C. E. *J. Comput. Chem.* **1990**, *11*, 105.
(8) Dunning, T. H. *J. Chem. Phys.* **1989**, *90*, 1007.
(9) Pople, J. A.; Binkley, J. S.; Seeger, R. *Int. J. Quantum Chem.* **1976**, *S10*, 1.
(10) Bartlett, R. J. *Annu. Rev. Phys. Chem.* **1981**, *32*, 359.
(11) Cizek, J. *Adv. Chem. Phys.* **1968**, *14*, 35.
(12) Cizek J.; Paldus, J. *Int. J. Quantum Chem.* **1971**, *5*, 359.
(13) Bartlett, R. J.; Purvis, G. D. *Int. J. Quantum Chem.* **1978**, *14*, 561; *Phys. Scr.* **1980**, *21*, 255.
(14) Nakatsuji, N.; Hirao, K. *J. Chem. Phys.* **1978**, *68*, 2053.
(15) Pople, J. A.; Krishnan, R.; Schlegel, H. B.; Binkley, J. S. *Int. J. Quantum Chem.* **1978**, *14*, 545.
(16) Jankowski, K.; Paldus, J. *Int. J. Quantum Chem.* **1980**, *18*, 1243.
(17) Chiles, R. A.; Dykstra, C. E. *Chem. Phys. Lett.* **1981**, *80*, 69.
(18) Dykstra, C. E.; Davidson, E. R. *Int. J. Quantum Chem.* **2000**, *78*, 226; Dykstra, C. E.; Liu, S.-Y.; Daskalakis, M. F.; Lucia, J. P.; Takahashi, M. *Chem. Phys. Lett.* **1987**, *137*, 266.
(19) Komornicki, A.; Dykstra, C. E.; Vincent, M. A.; Radom, L. *J. Am. Chem. Soc.* **1981**, *103*, 1652.
(20) Dykstra, C. E.; Jasien, P. G. *Chem. Phys. Lett.* **1984**, *109*, 388; Augspurger, J. D.; Dykstra, C. E. *J. Phys. Chem.* **1991**, *95*, 9230.
(21) Dykstra, C. E. *Adv. Chem. Phys.* **2003**, *126*, 1.
(22) Scheiner, S. *J. Am. Chem. Soc.* **1981**, *103*, 315.
(23) Del Bene, J. E.; Frisch, M. J.; Pople, J. A. *J. Phys. Chem.* **1985**, *89*, 3669.
(24) Frisch, M. J.; Del Bene, J. E.; Binkley, J. S.; Schaefer, H. F. *J. Chem. Phys.* **1986**, *84*, 2279.
(25) Del Bene, J. E. *J. Comput. Chem.* **1987**, *8*, 810.
(26) Lee, E. P. F.; Dyke, J. M. *Mol. Phys.* **1991**, *73*, 375.